Visual Analytics of Spatio-Temporal Uncertainties for Radiation Monitoring in a Nuclear Leakage Crisis

Haojin Jiang, Kui Yang, Yaqi Qin, Yifei Yang, Ying Zhao*, Fangfang Zhou

Central South University

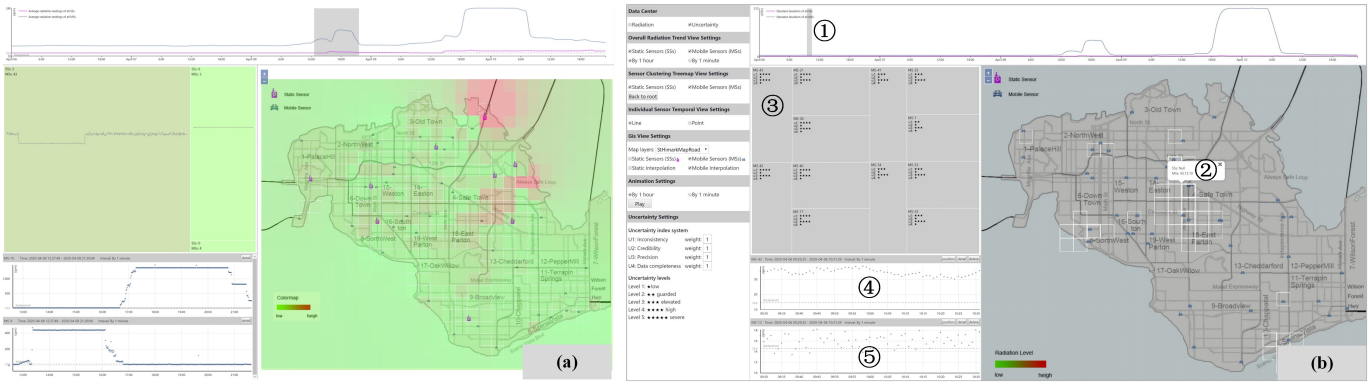

Fig.1: Interface overview. (a) The interface mainly shows the radiation information; (b) The interface mainly shows the uncertainty information.

ABSTRACT

Deployment of radiation sensor networks provides crucial information to ensure the safety of nuclear power plants. Due to the inherent uncertainty of spatio-temporal data from multi-types of sensors, it is equally important to evaluate both the radiation information and data confidence. This paper summarizes a visual analytics approach to analyze radiation levels and various types of uncertainty from interfaces representing either single aspects or integrated information.

1 INTRODUCTION

It is important to deploy effective sensor networks to ensure the safety of the nuclear power plant. For a wide coverage and high performance to cost, calibrated professional static sensors (SS) and homemade mobile sensors (MS) attaching to vehicles are in use. However, the difference on production standard inevitably engenders high uncertainties in spatio-temporal data, which directly undermines the reliability of analysis and application results. Effective visualizations can help understand complex uncertainties through carefully designed visualization views and interactions.

VAST Challenge 2019 MC2 simulated a potential nuclear crisis after an earthquake in St. Himark. The available data were mainly the radiation readings and related geo-locations for five days from SS and MS sensors around the city. Participants were required to use novel visualizations to analyze contamination conditions as well as data uncertainties.

This paper proposes an overview of our solution for MC2. The first part of our solution is a 6-step data processing. In particular, we provide feasible methods to define different types of uncertainty and perform a hierarchical system for assessment. Then an interactive interface with four visualization views is used for uncertainty comparison and contamination detection. The interface has three visualization modes. The three modes show the information about radiation (Fig.1(a)), uncertainty (Fig.1(b)), or the integration of both (Fig.2(b)) respectively. In particular, the four views are the two time-series views showing the global and detailed trend of readings from all sensors or individual sensors respectively, the treemap view for organizing cluster results and related uncertainty levels, and the GIS view for displaying spatial distribution of radiation and regional uncertainty.

* zhaoying@csu.edu.cn

2 DATA PREPROCESSING

We mainly preprocess the data in six steps.

Outlier detection. Since the noises in MS readings are sometimes indiscriminate from an important time-varying pattern which has continuous high values, we denoise them using LOF-ICAD algorithm combined with feature extraction.

Map layers generation. We design four map layers which can be freely overlaid representing neighborhoods, sensor locations, POIs and building types based on the background info and data analysis of MC1 and MC3.

Uncertainty classification and representation. We define four types of uncertainty to form an index system, including inconsistency, data completeness, credibility and precision. They can be quantified by different methods. Five qualitative levels of each index can be finally obtained after processing the quantitative results using a trapezoidal fuzzy membership function. And the overall levels of the system can be generated by AHP [1].

Pattern clustering. According to observation, certain time-varying patterns can provide insights of relevant triggering events. So we cluster sensors based on temporal patterns of readings, and organize the result using a treemap with rich visual encodings illustrated in Section 3.2.

Spatial interpolation. Given the insufficient spatial coverage of available data, we project radiation (coded by color) and uncertainty levels (coded by border thickness of regional grids) to the entire map by IDW spatial interpolation algorithm. In this way, regions without data have predictive values.

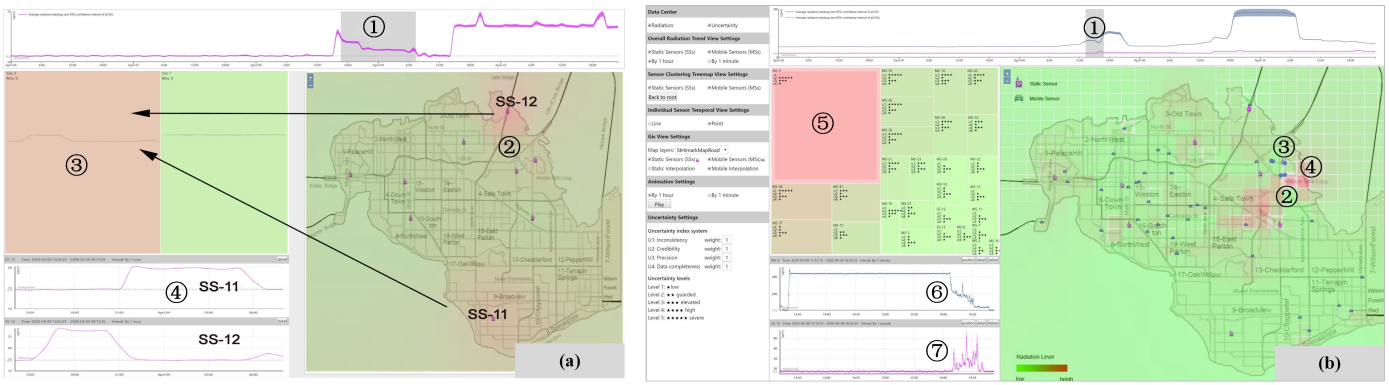

Fig.2: Case studies. (a) analysis of 2 SSs detecting notable high values; (b) conjoint analysis of radiation and uncertainty information to detect contaminated cars

3 VISUALIZATION

3.1 Overall Radiation Trend View

The global time-series chart shown on the top is designed to show the general variation trend of data from all sensors. It can depict the average or standard deviation of readings by hour from all SSs or MSs, representing the overall radiation level or data credibility over time. For a collaborative analysis of both aspects, the line denotes the average readings and the width of the band denotes the confidence interval with 95% coefficient. Users can select certain time period and other views will update correspondingly.

3.2 Sensor Clustering Treemap View

The sensor clustering treemap view is used to organize the pattern clustering results and the detailed levels of uncertainty. The root layer shows sensor clusters with a timeline in each rect representing the abstraction of time-varying patterns of a cluster. Click a rect to view the detailed information of individual sensors within the cluster, where specific levels of 4 uncertainty types are shown with the number of stars inside a rect. The radiation and overall uncertainty levels are represented by color and border thickness of a rect respectively.

3.3 Individual Sensor Temporal View

Individual sensor temporal view shows the detailed fluctuation of one sensor. It depicts the detailed readings by minute from individual sensors. Users can also click to see the raw readings for five days and freely add more plots by selecting sensor rects in the child layer of treemap. The view can also be clicked to show the relevant trajectories of a MS on the GIS view.

3.4 GIS View

The GIS View shows the spatial distribution of radiation levels and regional inconsistency around the entire city after interpolation. Similarly, the radiation levels are drawn by color coding and inconsistency levels are represented by border thickness of a regional grid. The pink and blue icons denote the current locations of SS and MS respectively. And users are welcome to overlay multiple map layers providing geo-information from different aspects.

All views are organized into one interface and support dynamic updating by animation, either by hour or by minute, which helps analysts to quickly know the change of situations over five days.

4 CASE STUDIES

4.1 Detect two contaminated locations

From the overall radiation trend view of static sensors, we found that the period (Apr 8 16:00-Apr 9 7:00) presented high radiation levels. After selecting that period (Fig.2(a)-1), we found the change related to the high radiation levels at the entrance of Jade Bridge and the Broadview on the map (Fig.2(a)-2). And these two locations could be verified in the treemap, where a cluster with SS-11 and SS-12 presented in red color displaying temporal spike pattern of readings (Fig.2(a)-3). When checking the two sensors in detailed time-series views, we can see that the readings from both sensors fell back to normal later (Fig.2(a)-4). Therefore, we highly suspect the two locations could be temporal parking spots of contaminated cars.

4.2 Inconsistency analysis of MS readings

From the overall radiation trend view, we selected the period (Apr 6 9:30-10:30) when there was no disruption from the earthquake (Fig.1(b)-1). From the map we can see the selected grids with thick borders where MS-13 and MS-10 passed by presented high inconsistency levels in radiation measurements (Fig.1(b)-2). In addition, MS-43 had a high inconsistency level with 4 stars (Fig.1(b)-3) and its readings were about 20 cpm higher than MS-13 (Fig.1(b)-4,5). Therefore, mobile sensors might have calibration issues and thus can be more unstable.

4.3 Detect contaminated cars movements

We selected the period (Apr 8 13:12-Apr 8 16:52) with high radiation readings (Fig.2(b)-1) when there could have been many contaminated cars. The regions around the Always Safe plant (AS) were high in both radiation and inconsistency levels and the treemap further demonstrated the red grids in AS loop were caused by high values detected by MS-9 (Fig.2(b)-2,4,5). From the individual sensor view, we found that the reading decline of MS-9 and reading increase of SS-15 at the entrance of AS loop (Fig.2(b)-3) occurred at almost the same time, which provides strong evidence of some contaminated cars driving away from AS (Fig.2(b)-6,7).

REFERENCE

[1] Fangfang Zhou, Xiaoru Lin, Xiaobo Luo, Ying Zhao, Yi Chen, Ning Chen and Weihua Gui. Visually Enhanced Situation Awareness for Complex Manufacturing Facility Monitoring in Smart Factories[J]. Journal of Visual Languages & Computing, 2017, 44(2):58-69.